Journal of Coastal Research	15	3	624–634	Royal Palm Beach, Florida	Summer 1999

Bedforms in a Laboratory Wave Flume: An Evaluation of Predictive Models for Bedform Wavelengths

S.W. Marsh†, C.E. Vincent†, and P.D. Osborne‡*

†School of Environmental Sciences
University of East Anglia
Norwich, NR4 7TJ

‡Scarborough College Coastal Research Group
University of Toronto
1265 Military Trail
Scarborough, Ontario,
Canada, M1C 1A4

ABSTRACT

MARSH, S.W.; VINCENT, C.E., and OSBORNE, P.D., 1999. Bedforms in a Laboratory Wave Flume: An Evaluation of Predictive Models for Bedform Wavelengths. *Journal of Coastal Research*, 15(3), 624–634. Royal Palm Beach (Florida), ISSN 0749-0208.

Recent bedform dimensions measured in shallow waters in the nearshore zone (VINCENT and OSBORNE, 1993; OSBORNE and VINCENT, 1993; MARSH, 1996) compare poorly with published predictive models for bedform dimensions. A series of experiments were conducted in a large flume with a computer-controlled wave generator and a sand bed, using waves of various amplitudes and characteristics including waves from a field site and monochromatic waves. The ripple wavelengths were then compared to the wavelengths predicted by the models of NIELSEN (1981), GRANT and MADSEN (1982), MOGRIDGE *et al.* (1994) and WIBERG and HARRIS (1994), and to the semi-quantitative model of CLIFTON (1976). Under spectral waves from the field site the mean ripple wavelengths are anorbital remaining constant (within the scatter of the measurements) and showing none of the trends predicted by the models but falling between the dimensions predicted by NIELSEN (1981) for 'laboratory' and 'field' waves. Under monochromatic waves the ripples scaled with the wave orbital amplitude ($\lambda = 0.4A_0$) and were much closer to the model predictions.

It is suggested that it is rather difficult to change the wavelength of ripples once they have formed. Field waves generally have a broad spectrum of frequencies (and hence of orbital excursions) so there is no length scale of sufficient dominance to force the bed to reform. With regular waves every orbital excursion is the same and the bed rapidly scales to this length. Our data suggest that bed form dimensions in an event may therefore be determined by the first waves capable of imposing their length scale on the bed, or by bed forms from an earlier event.

ADDITIONAL INDEX WORDS: *Ripple wavelength, spectral waves, monochromatic waves.*

INTRODUCTION

An understanding of how the sea bed responds to waves in relatively shallow water is crucial to generating realistic models for sediment movement. In particular, bedform geometry contributes to bed roughness (through form drag) and bedforms have a critical effect on the re-suspension of sediment through vortex roll up and ejection. Many empirical equations exist for predicting bedform geometry (*e.g.* CLIFTON (1976); NIELSEN (1981); WIBERG and HARRIS (1994); GRANT and MADSEN (1982), MOGRIDGE *et al.* (1994)). However, most of these are based on data from either deep water studies or from laboratory studies using artificial wave conditions. There is a paucity of data from shallow water (<2 metres). Instruments are now available that allow measurements of bedform geometry to be made in shallow water, with a relatively high degree of temporal and spatial resolution. The bedform dimensions measured during the BASEX (Bedforms And Suspension EXperiments) field experiments, on a macro-tidal beach in Cornwall, UK, where the water depth (at mean high water) varies from 2–3 m, compare poorly with published predictive models for bedform dimensions (VINCENT and OSBORNE (1993); OSBORNE and VINCENT (1993); MARSH (1996); VINCENT *et al.* (in press).

A series of experiments were conducted in a large wave flume at the Canadian National Research Council Laboratories (NRC), Ottawa, to try and explain why the results from previously-published equations compared so poorly with these field measurements. The wave conditions used in the flume varied from simulated, near-prototype scale waves, similar to those encountered in the Great Lakes, to nearly monochromatic wave trains. The bedform wavelength data provided a useful insight into the processes that occur beneath regular and irregular (natural) waves, helping to explain some of the divergence between models and field measurements. In this paper we compare the ripple wavelength models proposed by CLIFTON (1976), NIELSEN (1981), WIBERG and HARRIS (1994), GRANT and MADSEN (1982) and MOGRIDGE *et al.* (1994) to the new data from the NRC flume. Each of the five models considered predicts ripple wavelength based on measurements of hydrodynamic conditions.

97162 received 28 December 1997; accepted in revision 17 August 1998.

* Present Address: Division of Science and Technology—Geography, The University of Auckland, Tamaki Campus, Auckland, New Zealand.

PREVIOUS RESEARCH

The CLIFTON (1976) model is semi-quantitative; near-bed orbital velocity (U_m) and near-bed orbital velocity asymmetry (ΔU_m) are used to identify existence fields for different types of bedform.

$$U_m = 2\pi A_0/T,$$

where A_0 is the near-bed wave orbital-amplitude and T is wave period;

$$\Delta U_m = 14.8H^2/LT \sinh^4 kh$$

where H is wave height, L is wavelength, k is the wavenumber and h is water depth. Four bed states are then identified. 1. No Sediment Movement; 2. Symmetric Ripples; 3. Asymmetric Ripples and 4. Sheet Flow. The symmetric ripples are further divided into orbital, suborbital and anorbital ripples. The symmetric ripple range is of primary interest here, and has been further quantified by several studies including WIBERG and HARRIS (1994).

NIELSEN (1981) suggests that two equations are necessary to predict ripple wavelength λ; one for "field", the other for "laboratory" conditions.

$$\lambda/A_0 = \exp((693 - 0.37 \ln^7\psi)/(1000 + 0.75 \ln^8\psi))$$

for field conditions, and

$$\lambda/A_0 = 2.2 - 0.345\psi^{0.34}$$ for laboratory conditions,

where ψ is the mobility number

$$\psi = (A_0\omega)^2/(\rho_s - \rho)gD$$

A_0 is the near-bed wave orbital amplitude ($d_0/2$); ω is the wave radian frequency; ρ_s and ρ are the sediment and water densities respectively; g is acceleration due to gravity and D is the grain diameter. The distinction between "field" and "laboratory" conditions is interpreted here as being primarily due to the width of the wave spectrum; "field" conditions usually have relatively broad wave spectra (a wide spread of wave heights and periods), whereas "laboratory" conditions imply monochromatic wave spectra (i.e. series of waves that are identical with respect to height and period). Analyses of the bedform data from the first BASEX field experiment (VINCENT and OSBORNE (1993)) suggested that the equations proposed by NIELSEN (1981) act as bounding conditions for bedform geometry rather than a simple two value choice.

GRANT and MADSEN (1982) based their predictions of ripple wavelengths on the skin friction component of the boundary shear stress. An equilibrium range is proposed where ripple wavelength varies strongly with shear stress (but where steepness remains constant), followed at higher stresses by a break-off range where ripple wavelength does not depend as strongly on the boundary shear stress and where ripples become less steep as a flat bed is approached. The bedform geometry predictions are based on the laboratory tank data of CARSTENS *et al.* (1969).

WIBERG and HARRIS (1994) proposed that the anorbital ripple steepness η_{ano} should be determined iteratively using:

$$\frac{\eta_{ano}}{\lambda} = \exp\left[-0.95 \ln\left(\frac{2A_0}{\eta_{ano}}\right)^2 + 0.442 \ln\left(\frac{2A_0}{\eta_{ano}}\right) - 2.28\right]$$

where $\lambda = 535D$, for anorbital ripples. If $2A_0/\eta_{ano} > 100$ then ripples are actually anorbital while if $2A_0/\eta_{ano} < 20$ then the ripples are classified as orbital and have a predicted wavelength of $1.24A_0$. Between these two limits, ripples are classified as suborbital, and their wavelength is calculated using a weighted geometric mean between the limits of the orbital and anorbital ripple wavelength predictions.

The MOGRIDGE *et al.* (1994) model defines maximum ripple wavelengths using the value of a wave period parameter,

$$\chi = \frac{\rho D}{(\rho_s - \rho)T^2}$$

The wave period parameter is similar to the mobility number described above, except that it does not include a horizontal length term. In fact, $\chi(2A_0\pi)^2/\rho g D^2 = \psi$, the mobility number.

If $\chi > 0.15 \times 10^6$ ripple wavelength is grain size dependant with a value of 1394D. At lower values of χ, ripple wavelength is predicted using

$$\log_{10}(\lambda/D) = 13.373 - 13.772\chi^{0.02054}.$$

These five models were developed using different, but sometimes overlapping subsets of, the field and/or laboratory data of BAGNOLD (1946), MANOHAR (1955), INMAN (1957), YALIN and RUSSELL (1962), KENNEDY and FALCON (1965), HORIKAWA and WATANABE (1967), CARSTENS *et al.* (1969), MOGRIDGE and KAMPHUIS (1972), DINGLER (1974), DINGLER and INMAN (1976), LOFQUIST (1978), MILLER and KOMAR (1980a,b), NIELSEN (1981) and KOS'YAN (1988). They use the basic parameters of wave height, period, water depth, sediment diameter *etc.*, as predictors but there is a wide range in the ripple wavelengths predicted for a given set of hydrodynamic conditions. This problem is illustrated by much of the data presented below and shows the very real difficulties in selecting which models, if any, are the most appropriate for predicting bedforms under particular hydrodynamic conditions.

EQUIPMENT CONFIGURATION

Detailed measurements of both bedforms and suspended sediment concentrations were made during the wave flume experiment using two multi-frequency Acoustic BackScatter (ABS) systems. This paper focuses on bedform wavelength data collected using the ABS transducers mounted in two different configurations.

Acoustic transducers emit a short pulse of sound which can be scattered by any material of different acoustic impedance. In collection mode one, a transducer was mounted sub-horizontally close to the bed, in a "side-scan" mode. Any surface irregularities on the bed (bedforms) which have an elevation sufficient to breach the acoustic beam will cause sound to be reflected back to the transducer. By range-gating the returning (backscattered) signal through time, the positions of bedforms can be measured. In this series of experiments, two transducers were mounted 12 cm above the bed in a direction normal to the propagation of waves. The transducers were 1.1 m apart and each monitored a 1.2 m long section of the bed with a resolution of 1 cm. To achieve the best coverage over the maximum possible length of bed, the lowest fre-

Table 1. *Summary data for the natural wave drive signals, DE2 and DE5. Hydrodynamic conditions are summarized by wave height, H_{sig}, (m) and wave period, T_p, (sec) and near bed orbital amplitude, A_m, in water that is 1.8 m deep; bedform data are summarized by mean wavelength, λ, (m) and standard deviation, σ, (m).*

Gain Setting	Collection Mode	Wave Period (s)	Significant Wave Height (m)	Near Bed Orbital Amplitude (m)	Mean Ripple Wavelength (m)	Standard Deviation of Observed Ripple Wavelengths (m)
			Natural Wave Spectra			
DE2 0.4	1	3.2	0.24	0.10	0.18	0.05
DE2 0.6	1 and 2	3.3	0.36	0.16	0.16	0.05
DE2 0.8	1	3.3	0.48	0.21	0.21	0.06
DE2 1.0	1 and 2	3.2	0.57	0.24	0.24	0.05
DE5 0.5	1	3.4	0.42	0.21	0.16	0.03
DE5 0.75	1	3.6	0.58	0.31	0.15	0.03
DE5 1.0	1 and 2	4.0	0.86	0.53	0.20	0.08

quency transducer of each ABS system was used (as these have the widest beam angles); the frequencies were 1.97 MHz and 1 MHz. Side-scan profiles in subsequent sections show the backscattered acoustic pressure averaged over a one minute period.

In collection mode two, six transducers were mounted vertically on a mobile track above the bed. The transducers moved along the track over a 1.6 m length of bed, so that two dimensional profiles of bed elevation could be generated; this method is analogous to that used by DINGLER and INMAN (1976), and GREENWOOD *et al.* (1993). In this mode, the bed position is defined at the range bin containing the maximum acoustic return.

All sensors were mounted on a scaffolding frame that was suspended across the top of the flume. No structures were placed in, or on, the bed, thus eliminating any risk of physical disturbance of the bed by direct contact with hardware. Pressure cases housing the sensor electronics that operate the transducers were mounted above the water level on the top of the scaffolding frame, to minimise obstruction to the flow. These were connected to two PC-based logging systems.

The sand used for all experiments was commercial grade silica sand with a median grain size of 315 microns. The flume was covered with sand, to a depth of 15 cm, over a 10 m long section.

WAVE GENERATION AND WAVE SIGNALS USED

Waves were generated by a hydraulically driven, computer controlled paddle. The software used to control the paddle was the NRC GEDAP package (FUNKE *et al.*, 1980). This system allows a wide range of waves to be produced with a high degree of control. Wave reflections are damped by metal screens at the downwave end of the flume. Wave heights and periods in the vicinity of the instruments were monitored using capacitance wave wires; the water depth for all experiments was 1.8 m. Four different sets of wave conditions will be examined here.

1. The first set of conditions were created by simulating a broad spectrum of irregular wave conditions recorded in a field experiment by GREENWOOD *et al.* (1991). The signal is labelled the DE2 signal. The wave record was 20 minutes long, and could be repeated to allow longer periods of observation. Altering the gain on the wave generator causes changes in wave heights; the DE2 signal was played at four different gain settings (0.4, 0.6, 0.8 and 1.0). The resulting wave statistics are given in Table 1.

2. A single asymmetric wave group was extracted from the natural wave record (DE2) to create the DE5 drive signal. This wave group was repeated, both "forwards" and "backwards", at three different gain settings (0.5, 0.75 and 1) giving the wave conditions summarised in Table 1.

3. Symmetric bimodal wave groups (BIW) were generated artificially, by summing two monochromatic sets of wave heights and periods. The wave statistics of the resulting waves are shown in Table 2. The monochromatic waves used to generate the BIW signals are shown in Table 3.

4. Finally, monochromatic waves were used; these are referred to as the REG drive signals, all with a period of 3.6 (to match the peak period of the irregular wave series) seconds, and heights of 0.35 m, 0.8 m, and 0.92 m.

RESULTS

The DE2 drive signal was used at gain settings of 0.4, 0.6, 0.8 and 1, in both an increasing and decreasing sequence. Summaries of wave data and bedform measurements are shown in Table 1. Figure 1 shows a typical sequence of side-scan profiles for this wave signal. Peaks in backscattered acoustic pressure are clearly visible showing the location of the ripples. Figure 1 shows the bed after it had experienced half an hour of the DE2 waves at gain 0.4. All measurements quoted in the summary tables were taken after the bed had reached an "equilibrium" state. This was assessed visually whilst the waves were incident upon the bed; equilibration of the bed normally took 30 to 40 minutes from the time when the wave signal had first begun. Mean ripple wavelengths are plotted against near bed orbital amplitude in Figure 2; error bars on the measured ripple wavelengths are at ± 1 standard deviation. The predictions of the models introduced earlier are also shown on this figure. The NIELSEN (1981) field model (solid triangles) predicts that ripple wavelength will decrease as the near bed orbital diameter increases under these conditions, while all the other models suggest that ripple wavelength should scale positively with near bed orbital amplitude. The data show no significant correlation between the ripple wavelengths and near bed orbital amplitude for these hydrodynamic conditions. The best fit line through the data

Table 2. *Summary data for artificially generated bichromatic waves and monochromatic waves. Hydrodynamic conditions are summarized by wave height, H_{rms} (m) and wave period, T_p (sec) and near bed orbital amplitude, A_0, in water that is 1.8 m deep; bedform data are summarized by mean wavelength, λ, (m) and standard deviation, σ, (m).*

	Collection Mode	Wave Period (s)	Significant Wave Height (m)	Near Bed Orbital Amplitude (m)	Mean Ripple Wavelength (m)	Standard Deviation of Observed Ripple Wavelengths (m)
			Artifical Wave Spectra			
Bichromatic Drive Signals						
BIW_L4_H3	1	3.1	0.36	0.15	0.10	0.04
BIW_L4_H2	1	3.2	0.45	0.20	0.16	0.05
BIW_L4_H1	1	3.5	0.53	0.27	0.15	0.05
BIW_L4	1	3.3	0.67	0.32	0.14	0.06
BIW_L1	1	3.5	0.59	0.31	0.26	0.06
BIW_L2	1	3.1	0.63	0.27	0.17	0.02
BIW_L3	1	3.9	0.64	0.39	0.22	0.03
BIW_L6		3	0.68	0.27	0.14	0.05
Regular Drive Signals						
REG_1	2	3.6	0.35	0.19	0.12	0.03
REG_2	2	3.6	0.80	0.43	0.38	0.08
REG_3	2	3.6	0.92	0.49	0.34	0.11

points suggests that ripple wavelength decreases with near bed orbital diameter, but not as strongly as the NIELSEN (1981) model predicts. However the trend is not statistically significant at the 95% level.

The DE5 drive signal is made of repetitions of a single asymmetric wave group extracted from the DE2 drive signal. It was used at three different gain settings, in its original order and in reverse; no systematic differences in bed response were discerned for the DE5-forward and DE5-reverse signals. A sample of side-scan profiles from the DE5 signal at its lowest gain setting is shown in Figure 3. As the wave height was increased the bed forms became progressively more three dimensional, this results in the side scan profiles becoming more irregular. The ripple wavelength scales quoted here are, therefore, measured from a two dimensional slice in a wave normal direction along the bed. Summary data are shown in Table 1.

Figure 4 shows the ripple wavelength data plotted against near bed orbital diameter along with the model predictions for the DE5 drive signal. The NIELSEN (1981) field model (solid triangles) predicts that ripple behaviour will be conservative under these conditions while the NIELSEN (1981) laboratory based model (crosses) and the WIBERG and HARRIS (1994) model (asterisks) both predict that ripple wavelengths should reach a maximum length and then begin to decrease within the range of conditions experienced here. The MOGRIDGE *et al.* (1994) and the GRANT and MADSEN (1982) models (solid circles and solid squares respectively) both predict that ripple wavelengths will scale positively with near bed orbital amplitude. The observed mean ripple wavelengths show a statistically significant relationship between near bed orbital amplitude and measured ripple wavelength.

Table 3. *Summary data showing monochromatic wave heights and periods used in the generation of the BIW drive signals.*

	Monochromatic Waves Summed to give BIW Drive Signals			
Generation of Bichromatic Drive Signals	Wave Period 1 (sec)	Wave Height (m)	Wave Period (sec)	Wave Height (2) (m)
BIW_L4_H3	3.00	0.20	3.35	0.20
BIW_L4_H2	3.00	0.25	3.35	0.25
BIW_L4_H1	3.00	0.30	3.35	0.30
BIW_L4	3.00	0.35	3.35	0.35
BIW_L1	3.00	0.35	5.00	0.35
BIW_L2	3.00	0.35	4.00	0.35
BIW_L3	3.00	0.35	3.50	0.35
BIW_L6	3.00	0.35	3.18	0.35

The biwave (BIW) data span a wider range of near bed orbital diameters than the DE2 and DE5 drive signals. In some of the runs cross ripples were present, and the problem of taking measurements from a two dimensional slice of the bed is encountered. Summaries of wave statistics and the observed ripple wavelengths in the wave normal direction are given in Table 2. Ten minutes of sidescan ABS data from BIW-L1 are shown in Figure 5. This figure shows a dominance of larger scale features at the start of the run, followed by bedform reconfiguration to reveal smaller scale features in the final few minutes of data collection. To ensure systematic analysis, all measurements were made at the end of data collection. Figure 6 shows the bedform wavelength data and model predictions for the biwave runs. The model predictions do not all follow smooth lines on this figure because the relationship between wave height and wave period is not the same for all runs. For the DE2 and DE5 wave signals, the wave characteristics were adjusted simply by changing the gain on the wave generator; for the Biwave signals, wave periods and wave heights are controlled independently. The data show that bedform wavelengths scale positively with near bed orbital amplitudes, but most length scales are over predicted by the previously published models. Only the NIELSEN (1981) field model (solid triangles), which was developed for broader wave spectra, under-predicts ripple wavelengths for these waves.

Three sets of monochromatic waves were used in the ex-

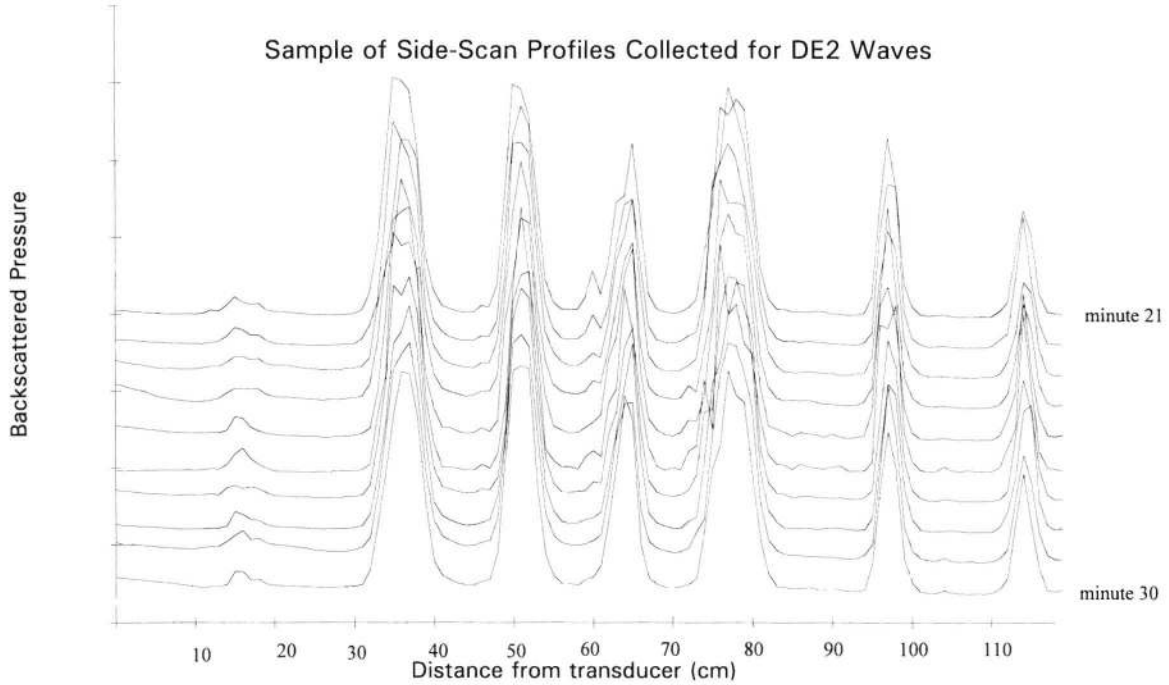

Figure 1. Ten minutes of side-scan profiles collected at the end of thirty minutes of the DE2 drive signal at gain 0.4.

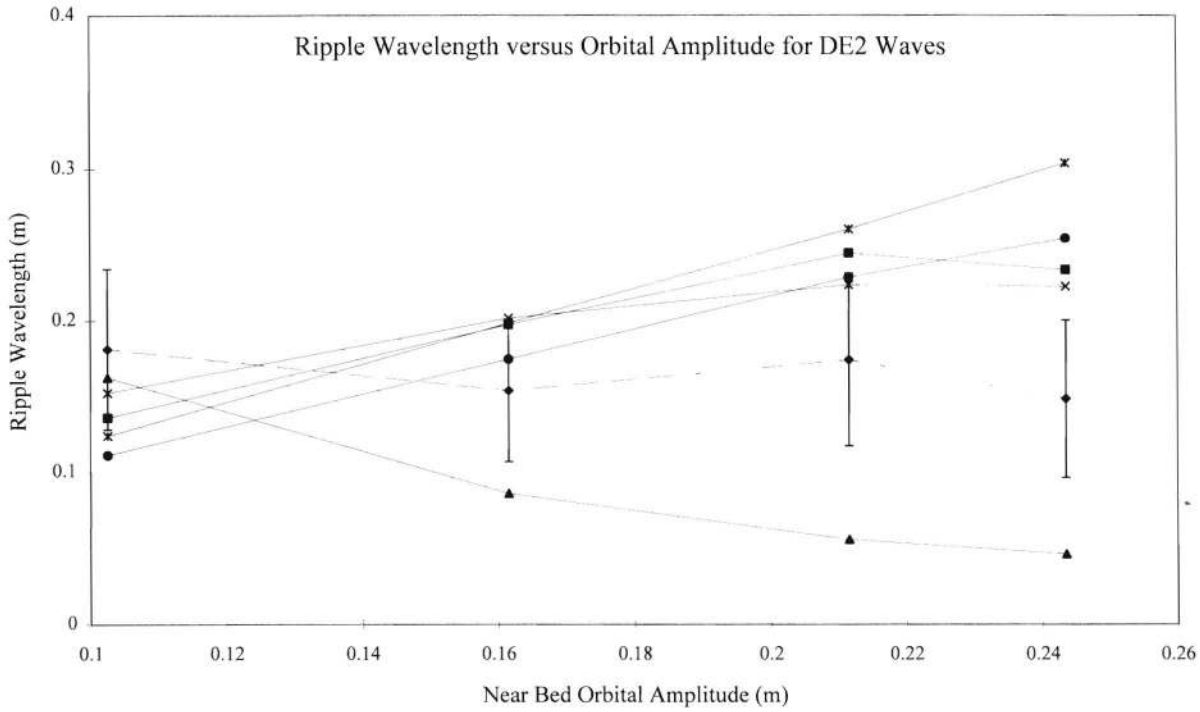

Figure 2. Ripple wavelengths for the DE2 drive signals, at each near bed orbital amplitude. Data (mean measured ripple wavelength)—diamonds. Model predictions: Grant and Madsen—squares; Nielsen (field)—triangles; Nielsen (laboratory)—crosses; Wiberg and Harris—asterisks, and Mogridge *et al*—circles versus near bed orbital amplitude for the DE2 drive signal.

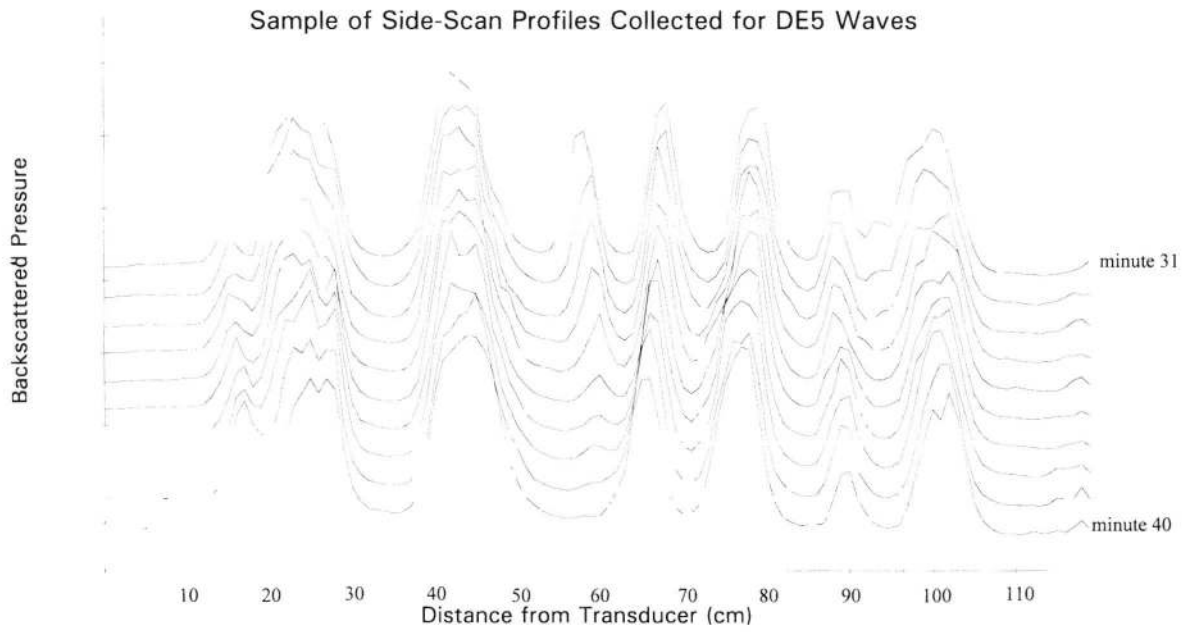

Figure 3. Ten minutes of side scan profiles collected at the end of forty minutes of the DE5 drive signal at gain 0.5.

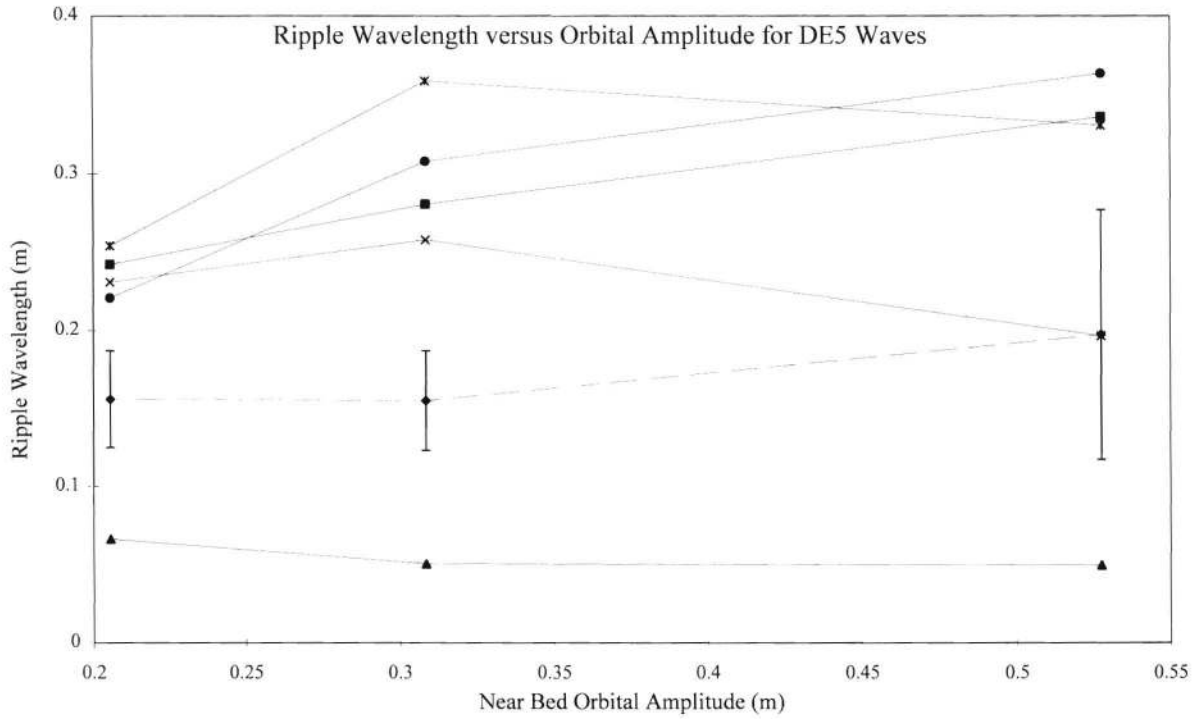

Figure 4. Ripple wavelengths for the DE5 drive signals, at each near bed orbital amplitude. Data (mean measured ripple wavelength)—diamonds. Model predictions: Grant and Madsen—squares; Nielsen (field)—triangles; Nielsen (laboratory)—crosses; Wiberg and Harris—asterisks, and Mogridge *et al.*—circles versus near bed orbital amplitude for the DE2 drive signal.

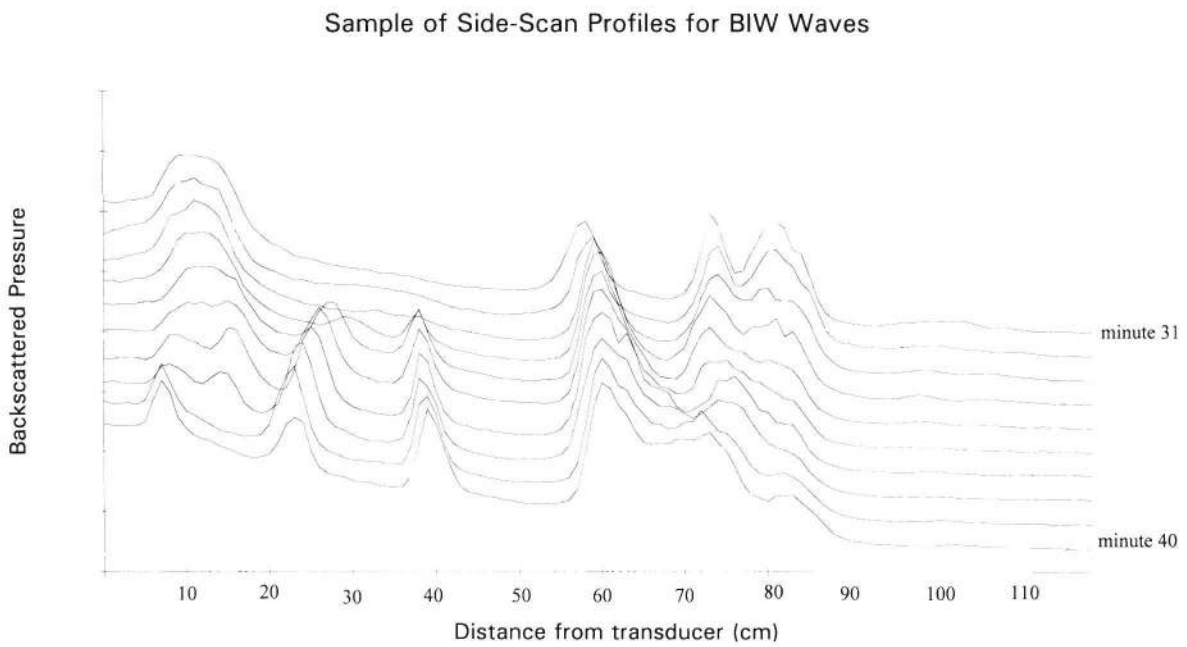

Figure 5. Ten minutes of side scan collected at the end of forty minutes of the BIW_L1 drive signal.

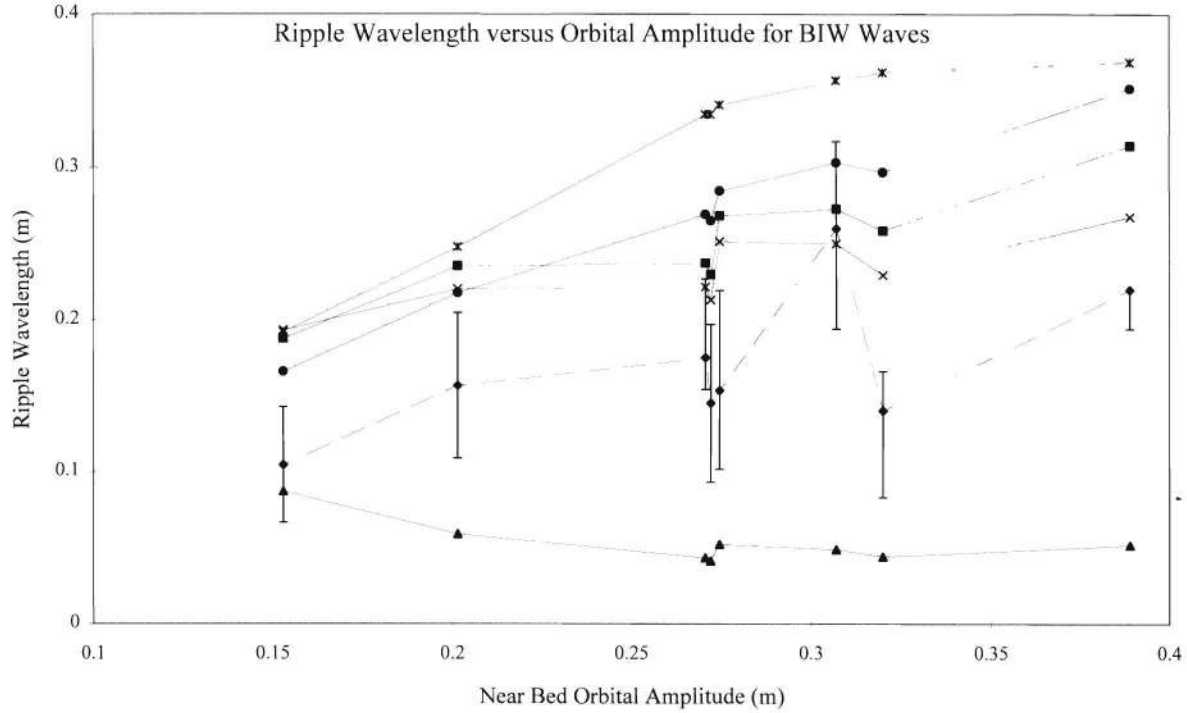

Figure 6. Ripple wavelengths for the Bichromatic Wave drive signals, at each near bed orbital amplitude. Data (mean measured ripple wavelength)—diamonds. Model predictions: Grant and Madsen—squares; Nielsen (field)—triangles; Nielsen (laboratory)—crosses; Wiberg and Harris—asterisks, and Mogridge *et al.*—circles versus near bed orbital amplitude for the DE2 drive signal.

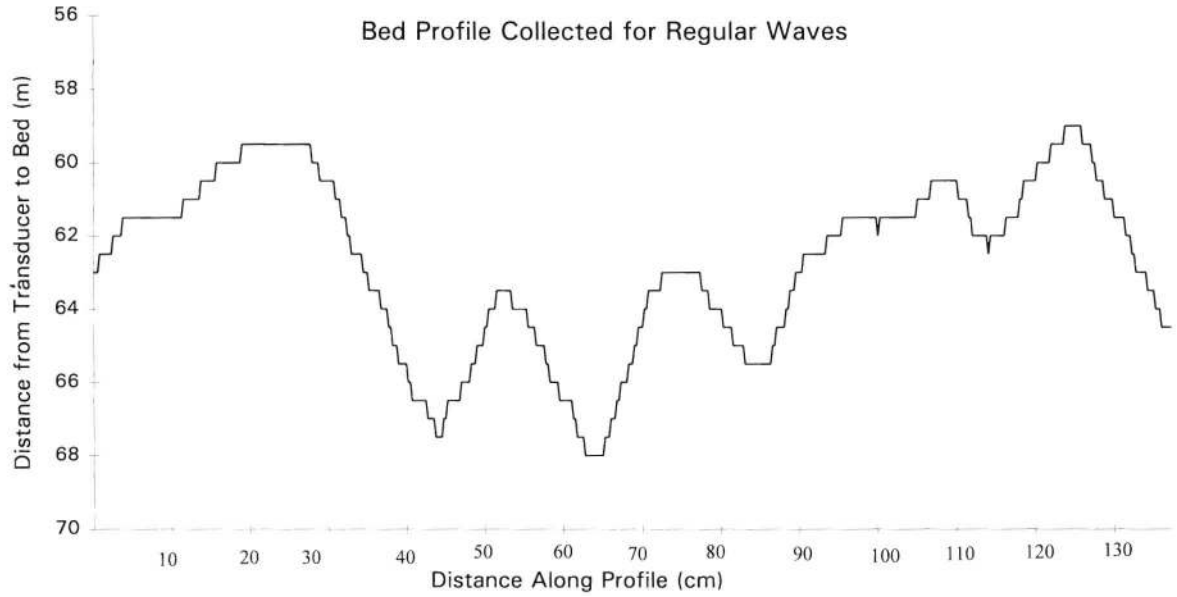

Figure 7. Bed profiles collected using collection mode2 for the regular wave drive signals. Profiles collected after 1 hour of waves; waves turned off during data collection.

periment. These all had a wave period of 3.6 seconds; wave height was increased from 0.35 m through 0.8 m to 0.92 m. All data were collected using collection mode two. Summary data are provided in Table 2. A sample of typical bed profiles are shown in Figure 7. These were collected after the wave generator had been switched off, so it is possible that the bedforms may have "relaxed" slightly. This is unlikely to affect the length scales quoted, but the vertical component of the profiles shown may not be identical to the bed profile when waves were present. Again the bedforms became three dimensional at large orbital amplitudes and the problem of taking two dimensional measurements from a three dimensional bed was encountered. As above the length scales quoted here are those in a wave-normal direction.

Figure 8 suggests that bedform length scales are far more responsive to changes in near bed orbital diameter beneath these waves than beneath the previous wave signals. Beneath the smallest waves, the bedforms observed are rather smaller than all the model predictions, except the NIELSEN (1981) field model (solid triangles). When the wave height is increased to 0.8 m, with a near bed orbital amplitude of 0.43 m, the bedform length scale increases to a greater length than any of the models predict. As the wave height is increased even further the observed bedform wavelength decreases slightly; however, so few ripples are covered by the 1.6 m track that the difference is well within the uncertainty of the measurements. Nonetheless the decrease in ripple wavelength at these higher orbital amplitudes is in qualitative agreement with the NIELSEN (1981) laboratory-based model (crosses), and is an almost exact agreement with the WIBERG and HARRIS (1994) model (asterisks).

DISCUSSION AND CONCLUSIONS

A weakness of several of the quantitative models is that they imply two dimensional bedforms. The Clifton model suggests that ripple asymmetry and the onset of three-dimensionality can be distinguished using maximum flow velocity and flow velocity asymmetry determined by second order wave theory (ADEYOMO, 1970). It was noted above that during several runs the bed became three dimensional. Figure 9 shows a general difference in the existence fields for 2D and 3D bed states, with 3D bed states not being observed in this study when the velocity assymmetry is less than approximately 8 cm per second.

The bedform wavelength data are summarised by best fit lines through the data presented earlier; these are shown in Figure 10. The closest we were able to come to field conditions in this series of experiments was the DE2 drive signal. The bedforms generated by these waves show no significant scaling of ripple wavelength with near bed orbital diameter. However as the waves used to generate the bedforms become increasingly "regular", firstly by using just a single wave group from the DE2 signal (DE5) and then through bi-wave to monochromatic wave states there is an increase in the dependence of bedform wavelengths on near bed orbital diameter. Although only three near bed orbital amplitudes are available for regular wave conditions from this experiment, the linear best fit through this data is $\lambda \approx 0.4\ A_0$. This is consistent with several earlier studies which quote $\lambda = 0.3 \rightarrow 0.5A_0$ (*e.g.*, INMAN (1976); WIBERG and HARRIS (1994); MILLER and KOMAR (1980a)).

The data begin to explain why so many model predictions have been found to be unsuccessful in field situations. Sev-

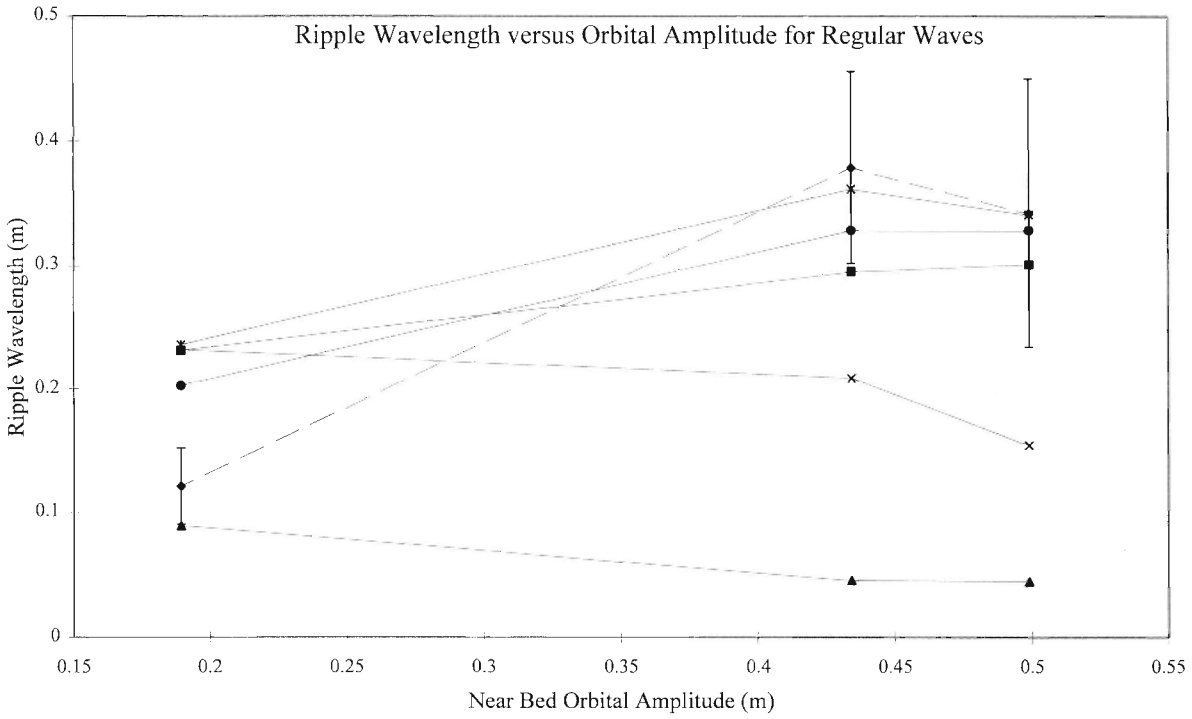

Figure 8. Ripple wavelengths for the Regular Wave drive signals, at each near bed orbital amplitude. Data (mean measured ripple wavelength)—diamonds. Model predictions: Grant and Madsen—squares; Nielsen (field)—triangles; Nielsen (laboratory)—crosses; Wiberg and Harris—asterisks, and Mogridge *et al.*—circles versus near bed orbital amplitude for the DE2 drive signal.

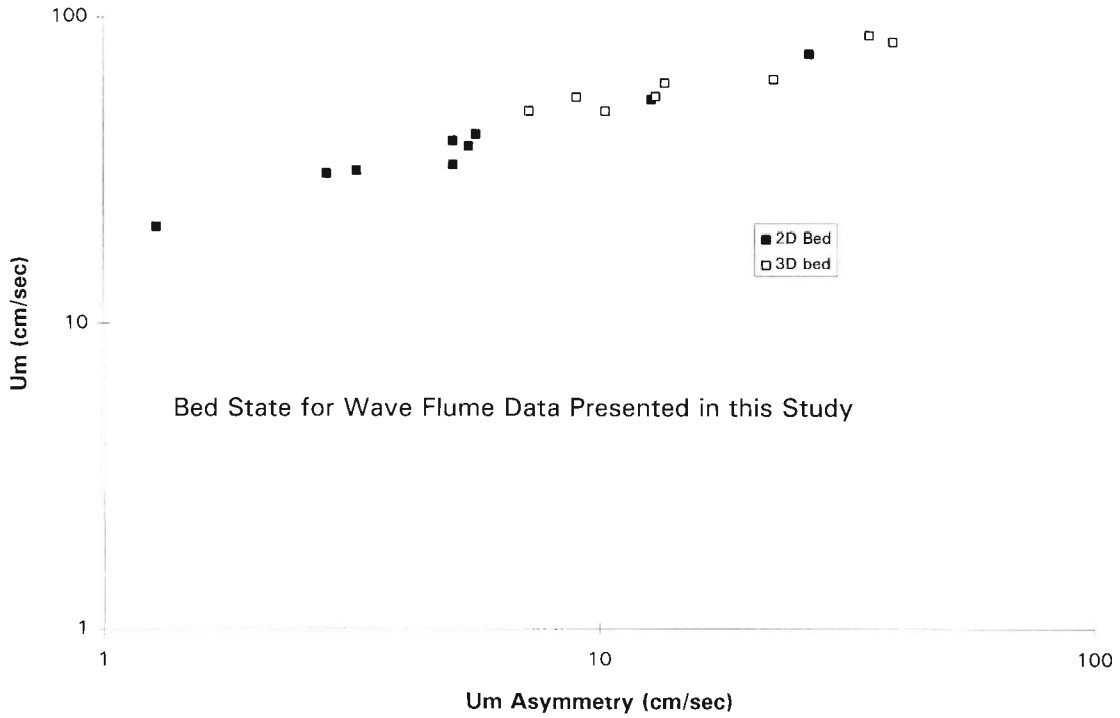

Figure 9. Classification of bed state using flow velocity and flow asymmetry.

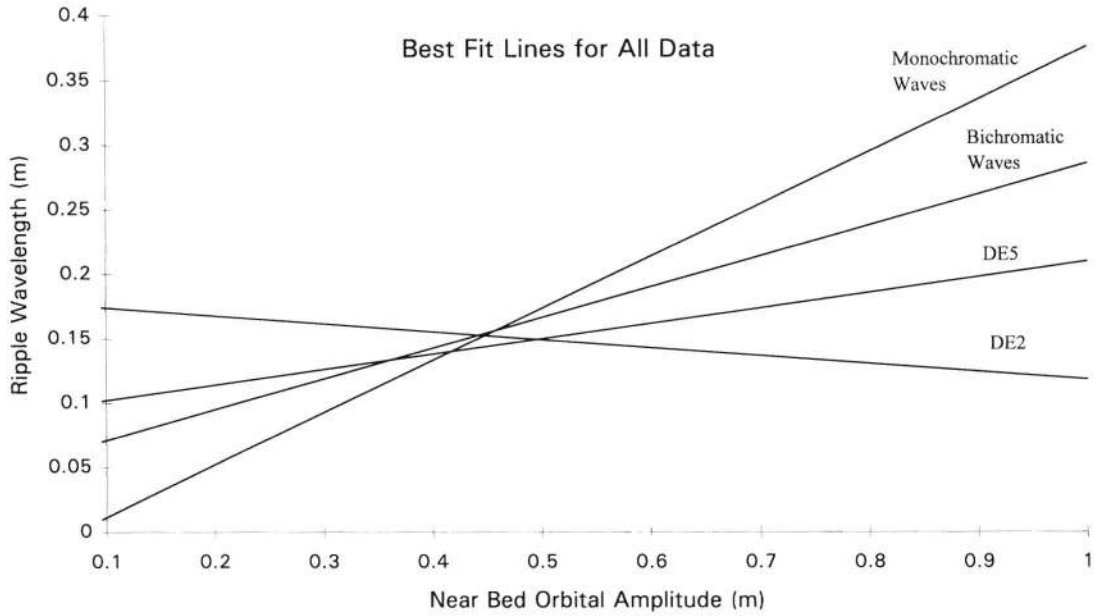

Figure 10. Summary best fit lines through all data. For DE2 data $\lambda = -0.06A_0 + 0.18$, from 67 ripple wavelength measurements, not statistically significant. For DE5 $\lambda = 0.12A_0 + 0.09$, from 60 ripple wavelength measurements, significant at 95%; for the bichromatic waves $\lambda = 0.23A_0 + 0.05$, from 63 ripple wavelength measurements, significant at 95%; for the regular waves $\lambda = 0.40A_0 - 0.03$, from 18 ripple wavelength measurements, significant at 95%.

eral of the models tested here contain a bias towards laboratory data, even though they have been put forward for use in field situations. The GRANT and MADSEN (1982) model, for instance, is based largely on the laboratory data of CARSTENS *et al.* (1969). The data from this study suggest that the NIELSEN (1981) approach is correct, in drawing a distinction between laboratory data and field data. This study, though, shows that there may be a range of bedform dependencies on hydrodynamic conditions which vary with the spectral width of waves incident upon an area. In fact the distinction drawn by NIELSEN (1981) is a manifestation of the fact that laboratory data have historically been collected under conditions of monochromatic waves, whilst field studies have presented data from broad banded wave spectra.

If this is the case, is it possible to explain why waves in the field (generally with broad wave spectra), do not exert a strong control on bedforms? The generally accepted use of significant wave height ($H_{1/3}$) and period to characterise the wave field is inadequate to describe the *range* of wave heights and periods in the wave field. If we hypothesise that the ripples will generally scale with near-bed wave orbital excursion then waves with a broad spectrum will contain a wide range of such scales. If the sea bed is initially flat and the waves are suddenly switched on (the normal laboratory scenario) then the bed is likely to scale with the orbital excursion of the waves around the significant wave height. In the sea, the sea surface and the sea bed are rarely flat, the bed exhibiting "relict" bedforms even when the local wave field is incapable of moving sediment, and waves generally build from small to large waves. Hence the waves are usually acting to change an existing ripple field; to change the wavelength of a ripple field even by a small amount requires a reconfiguration of the sea bed involving considerable movement of sediment (MARSH (1996)).

When the waves are regular (as in many laboratory flume experiments) every wave acts to impose the same scale on the bed and (as shown with the REG signal) the bed reconfigures. For a broad spectrum, no such single scale exists and the ripple field cannot respond except by maintaining its existing wavelength; we speculate that the effect of the few waves which scale to the existing bedforms have a greater influence in re-establishing the bedforms than the majority which act, individually, to reconfigure the bed. If true, the bed history is as important as the hydrodynamic conditions in determining bedform geometry. The waves produced by the DE2 signal (the signal from a field site), varying through a cycle of gains, mimic the changes in wave energy during a storm, but the bedform wavelengths do not vary significantly as the wave spectrum is broad.

In relatively shallow water conditions it is, therefore, very difficult to predict wavelengths of bedforms without a detailed knowledge of the spectral characteristics of the incident wave field and the bed history. Previously published models tend to include an implicit assumption that the bed will be highly dynamic. This results in model predictions often being rather poor for data collected in shallow water under varying hydrodynamic conditions. It is generally accepted that there is a time lag between the onset of a given set of hydrodynamic conditions and the development of 'equilibrium' bedforms, but the timescales concerned are poorly understood. It is also assumed that the highest one-third of the waves are crucial to the development of new bedform length

scales. The data presented here and those from previous studies, show that where spectral width is narrow, the time lag necessary for bedform equilibrium to occur is likely to be short. However as the spectral width increases, the bedform equilibration time will also increase. Under natural, irregular wave spectra it is possible that bedforms will be in equilibrium with waves in the spectra that are smaller than the largest one-third of the waves. Under these conditions the characteristic length scale of bedforms may remain largely unchanged despite apparent changes in hydrodynamic conditions calculated using H_{sig}. This type of bed response is discussed in VINCENT and OSBORNE (1993), and is described in greater detail in MARSH (1996). It is suggested that future work regarding bedforms should pay close attention to waves throughout the whole spectra, and not just those that make up the largest one-third.

ACKNOWLEDGEMENTS

The wave flume experiment was co-ordinated by Prof. B. Greenwood, University of Toronto. A large team of scientists were involved in data collection. M. Webb (UEA), C. Boldy (U. Toronto), K. Jagger (U. Toronto), X. Zhiming (U. Toronto) helped with equipment installation and operation of data logging equipment. M. Miles, M. Davies and D. Willis from the NRC made the wave flume available. Stephen Marsh was supported by a NERC studentship.

LITERATURE CITED

ADEYOMO, M.D., 1970. Velocity fields in the wave breaker zone, *Proceedings 12th Conference Coastal Engineering*. (ASCE), Pp. 435–460.

BAGNOLD, R.A., 1946. Motion of waves in shallow water: Interaction between waves and sand bottom: *Proceedings Royal Society London*. A., 187, 1–15.

CARSTENS, M.R.; NEILSON, F.M., and ALTINBILEK, H.D., 1969. Bed forms generated in the laboratory under an oscillatory flow: Analytical and experimental study: *U.S. Army Corps of Engineers, Coastal Engineering Research Centre, Technical Memorandum*. No. 28, 39p.

CLIFTON, H.E., 1976. Wave-formed sedimentary structures—A conceptual model. *In:* DAVIS, R.A. and ETHINGTON, R.L. (eds.), *Beach and Nearshore Sedimentation.*, SEPM Special Publication No. 24.

DINGLER, J.D., 1974. Wave Formed Ripples in Nearshore Sands Ph.D. thesis, 136p. San Diego, University California.

DINGLER, J.R. and INMAN, D.L., 1976. Wave formed ripples in nearshore sands. *Proceedings 15th Coastal Engineering Conference American Society Civil Engineers*. (New York), Pp. 2109–2126

FUNKE, E.R.; CROOKSHANK, N.L., and WINGHAM, M., 1980. An introduction to GEDAP—an integrated software system for experimental control, data acquisition and data analysis. *Technical Republic LTR-HY-75*, Institute Mechanical Engineering, NRC Canada.

GRANT, W.D. and MADSEN, O.S., 1982. Moveable bed roughness in unsteady oscillatory flow. *Journal Geophysical Research*, 87, 469–481.

GREENWOOD, B.; OSBORNE, P.D., and BOWEN, A.J., 1991. Measurements of suspended sediment transport: Prototype shorefaces, *Proceedings Coastal Sediments '91*, (ASCE Conf. Seattle 1991), Pp. 284–299.

GREENWOOD, B.; RICHARDS, R.G., and BRANDER, R.W., 1993. Acoustic imaging of sea-bed geometry: A high resolution remote tracking sonar (HRRTS II), *Marine Geology* 112, 207–218.

HORIKAWA, K. and WATANABE, A., 1967. A study on sand movement due to wave action. *Coastal Engineering Japan*, 10, 39–57.

INMAN, D.L., 1957. Wave-generated ripples in nearshore sands: *U.S. Army Corps of Engineers Beach Erosion Board Technical Memo*, No. 100, 67p.

KENNEDY, J.F. and FALCON, M., 1965. Wave Generated Sediment Ripples: *Massachusetts Institute Technology, Hydrodynamics Lab, Report*, Cambridge, No. 86, 86p.

KOS'YAN, R.D., 1988. On the dimensions of passive ripple marks in the nearshore zone, *Marine Geology*, 80, 149–153.

LOFQUIST, K.E.B., 1978. Sand-ripple growthin an oscillatory-flow water tunnel: *U.S. Army Corps of Engineers, Coastal Engineering Research Centre, Technical Paper* 78–5.

MANOHAR, M., 1955. Mechanics of bottom sediment movement due to wave action. *U.S. Army Corps of Engineers, Beach Erosion Board, Tech Memorandum*, 75.

MARSH, S.W., 1996. A Study of Bedforms and Suspended Sediments Using Acoustic Backscatter Instrumentation, PhD thesis, 295p., University of East Anglia, Norwich, UK.

MOGRIDGE, G.R.; DAVIES, M.H., and WILLIS, D.H., 1994. Geometry prediction for wave generated bedforms. *Coastal Engineering*. (22), 255–286.

MILLER, M.C. and KOMAR, P.D., 1980a. Oscillation sand ripples generated by laboratory apparatus. *Journal Sedimentary Petrology*. 50(1), 173–182.

MILLER, M.C. and KOMAR, P.D., 1980b. A field investigation of the relationship between oscillation ripple spacing and the near-bottom water orbital motions. *Journal Sedimentary Petrology*, 50(1), 183–191.

MOGRIDGE, G.R. and KAMPHUIS, J.W., 1972. Experiments on bed form generation by wave action. *Proceedings 13th Coastal Engineering*, (Vancouver), Vol II, Pp. 1123–1142.

NIELSEN, P., 1981. Dynamics and geometry of wave-generated ripples. *Journal Geophysical Research*, 86(C7), 6467–6472.

OSBORNE, P.D. and VINCENT, C.E., 1993. Dynamics of large and small-scale bedforms on a macrotidal shoreface under shoaling and breaking waves, *Marine Geology*, 115 (3-4); 207–226.

VINCENT, C.E. and OSBORNE, P.D., 1993. Bedform Dimensions and Migration Rates Under Shoaling and Breaking Waves. *Continental Shelf Research*, 13(11), 1267–1280.

VINCENT, C.E.; MARSH, S.W.; WEBB, M., and OSBORNE, P.D. (under review). Spatial and temporal structures of suspension and transport over mega-ripples on the shore face. *Journal Geophysical Research*.

WIBERG, L. and HARRIS, C.K., 1994. Ripple geometry in wave dominated environments. *Journal Geophysical Research*. 99 C1, 775–789.

YALIN, M.S. and RUSSELL, R.D.H., 1962. Similarity in sediment transport due to waves. *Proceedings 8th Conference Coastal Engineering*, (ASCE), Pp. 151–171.